

# Scalar field haloes as gravitational lenses

Franz E. Schunck<sup>1</sup>, Burkhard Fuchs<sup>2</sup> & Eckehard W. Mielke<sup>3</sup>

<sup>1</sup>*Institut für Theoretische Physik, Universität zu Köln, 50923 Köln, Germany*

<sup>2</sup>*Astronomisches Rechen-Institut, Mönchhofstr. 12–14, 69120 Heidelberg, Germany,*

<sup>3</sup>*Departamento de Física, Universidad Autónoma Metropolitana–Iztapalapa, Apartado Postal 55-534, C.P. 09340, México, D.F., México*

Accepted Received ; in original form 2005

## ABSTRACT

A non-topological soliton model with a repulsive scalar self-interaction of the Emden type provides a constant density core, similarly as the empirical Burkert profile of dark matter haloes. As a further test, we derive the gravitational lens properties of our model, in particular, the demarcation curves between ‘weak’ and ‘strong’ lensing. Accordingly, strong lensing with typically three images is almost three times more probable for our solitonic model than for the Burkert fit. Moreover, some prospective consequences of a possible flattening of dark matter haloes are indicated.

**Key words:** dark matter, gravitational lensing, galaxies: kinematics and dynamics

## 1 INTRODUCTION

Real scalar fields could provide mutual connections between cosmology and particle physics. The first attempt to admit a gravity scalar was by Nordström (1913), whereas Jordan (1959) as well as Brans & Dicke (1961) introduced it as a means for varying the gravitational ‘constant’  $G$  with time. The most intensive application of scalar fields occurs in the early universe scenarios. A prime example is inflation driven by the potential energy of the real scalar field, the inflaton, and in phase transitions together with the production of topological defects (Vilenkin & Shellard 1994). It also arises in the theories of superstrings where the dilaton couples universally to the trace of the energy-momentum tensor and leads to the so-called superinflation driven by the kinetic energy of the scalar field (see Gasperini & Veneziano 1993a, 1993b).

One of the main predictions of general relativity (GR) is the *deflection of light* in gravitational fields of compact objects known as *gravitational lensing*. Although the deflection of light by the Sun, up to a factor *of two*, was suggested by Soldner already in 1801 in the context of Newton’s theory, the correct value of  $\delta = 4M_{\odot}/R_{\odot} \simeq 1.75''$  was derived within the framework of general relativity by Chwolson (1924) and Einstein (1936), see Schneider et al. (1992) for more details. Intensive studies of gravitationally lensed objects began with the observation (Young et al. 1980) of the double quasar Q0957+561 with redshift  $z = 0.39$  and were mainly concentrated on the weak gravitational lensing effect for which the deflection is very small, up to a few arcseconds (see Bartelmann & Schneider 2001 for a recent review). In general, one can distinguish between lensing on non-cosmological and cosmological distances. As for the former one can have lensing by a star of solar mass  $M_{\odot}$  in a

galaxy with the deflection angles of the order of milliarcseconds and by a galaxy of  $10^{11} M_{\odot}$  with the deflection angles of the order of arcseconds. Although model-dependent luminosity distances have to be assumed, this provides us with the opportunity to determine the mass distribution of dark matter haloes, in particular the inner density slopes. Moreover, information on the cosmological parameters such as the Hubble constant  $H_0$ , the deceleration parameter  $q_0$  and the cosmological constant  $\Lambda$  (Fukugita et al. 1990), can be obtained.

In the case of weak lensing, a comparison with Newton’s theory is instructive, but all the Newtonian-based intuition fails for the cases of the large deflection angles. If one has a black hole, or a strong compact object such as a neutron star, then the gravitational lensing effects have to be treated in fully relativistic terms (Petters 2003). The deflection angles can be of the order of degrees allowing the light to orbit the lens several times such that multiple images can be formed (Cramer 1997, Dabrowski & Schunck 2000). These effects are especially interesting for accretion disks (Peitz & Appl 1997). It is worth mentioning the possibility of gravitational lensing by exotic matter such as cosmic strings (Vilenkin & Shellard 1994), boson stars (Schunck & Mielke, 1999, 2003) and by gravitational waves (Faraoni 1993).

Recently, Virbhadra et al. (1998, 2002) coupled a real massless scalar field to the Einstein equations and got a general static spherically symmetric asymptotically flat solution with a naked singularity which, apart from mass, has an extra parameter called “scalar charge”. They found a possibility of having four images of a source at the observer position together with a double *Einstein ring*.

In this paper, we investigate the gravitational lensing of a spherically symmetric halo constructed from an exactly solvable scalar field model with a *self-interaction* of the Em-

den type. To some extent this adopts the proposal of Spergel & Steinhardt (2000) that dark matter (DM) could be weakly self-interacting, or even a Bose-Einstein condensate (Goodman, 2000) with a repulsive potential. Then, DM would be more ‘collisional’ and may avoid the central cusps of the conventional cold dark matter (CDM) haloes.

The paper is organized as follows. In Section 2 we study the photon trajectories arising from null geodesics in the gravitational field of a spherically symmetric halo. In Section 3 we derive the density profile of our non-topological soliton (NTS) model and compare it with other empirical profiles, such as the quasi-isothermal sphere or the Burkert fit. The rotation curves derived for the NTS halo in Section 4 are contrasted to those emerging from the isothermal sphere and the Burkert fit. In Section 5, we discuss the effects of gravitational lensing by such bosonic configurations, calculate exactly the normalized projected mass, corrections due to pressure, and draw the dimensionless weak-field lens equation. Demarcation curves between ‘weak’ and ‘strong’ lensing for the NTS halo are compared with those of other prominent models in Section 6. The location of Einstein rings, the image separation and magnification are provided in Section 7. Section 8 summarizes the results and gives an outlook on the consequences of a possible flattening of NTS haloes.

## 2 PHOTON TRAJECTORIES IN A GRAVITATIONAL FIELD

For reasons mentioned in the introduction gravitational lensing requires a full *general-relativistic framework*:

For spherically symmetric halo, the line element reads

$$ds^2 = e^{\nu(r)} dt^2 - e^{\tilde{\lambda}(r)} dr^2 - r^2 (d\vartheta^2 + \sin^2 \vartheta d\varphi^2), \quad (1)$$

in which the functions  $\nu = \nu(r)$  and  $\tilde{\lambda} = \tilde{\lambda}(r)$  depend on the Schwarzschild type radial coordinate  $r$ .

The main point of our analysis is the gravitational lensing properties by a bosonic halo and this requires the discussion of trajectories of photons along a null geodesics in the plain  $\vartheta = \pi/2$ . It is equivalent to the energy conservation

$$\frac{1}{2} \left( \frac{dr}{d\tau} \right)^2 + V_{\text{eff}} = \frac{1}{2} F^2 e^{-\tilde{\lambda}-\nu} \quad (2)$$

of a particle with kinetic energy moving in the effective gravitational potential

$$V_{\text{eff}} = e^{-\tilde{\lambda}} \frac{L^2}{2r^2}. \quad (3)$$

Here  $F := e^\nu dt/d\tau$  is the total energy,  $L := r^2 d\varphi/d\tau$  the angular momentum of the photon, and  $\tau$  an affine parameter along null geodesics, such that  $L/F = r^2 e^{-\nu} d\varphi/dt = r e^{-\nu/2}$ .

When the light travelling from a source is deflected by a halo, the deflection angle is given by (Sextl & Urbantke 1983, p. 110)

$$\hat{\alpha}(r_0) = 2 \int_{r_0}^{\infty} \frac{be^{\tilde{\lambda}/2}}{\sqrt{r^2 e^{-\nu} - b^2}} \frac{dr}{r} - \pi, \quad (4)$$

where

$$b = L/F(r_0) = r_0 \exp[-\nu(r_0)/2], \quad (5)$$

is the impact parameter and  $r_0$  the closest distance between a light ray and the center of the halo for which  $V_{\text{eff}}(r_0) = (F^2/2) \exp[-\nu(r_0) - \tilde{\lambda}(r_0)]$  holds.

The diagonal components of the energy-momentum tensor  $T_\mu{}^\nu(\Phi) = \text{diag}(\rho, -p_r, -p_\perp, -p_\perp)$  of a scalar field are

$$\begin{aligned} \rho &= \frac{1}{2} \left( \omega^2 P^2 e^{-\nu} + P'^2 e^{-\tilde{\lambda}} + U \right), \\ p_r &= \rho - U, \\ p_\perp &= p_r - P'^2 e^{-\tilde{\lambda}}. \end{aligned} \quad (6)$$

which, due to  $\nabla^\mu T_\mu{}^\nu = 0$ , satisfy the *generalisation*

$$\frac{d}{dr} p_r = -\nu' \left( \rho + p_r - \frac{2}{r} (p_r - p_\perp) \right) \quad (7)$$

of the Tolman-Oppenheimer-Volkoff equation for an anisotropic ‘fluid’, cf. Schunck & Mielke (2003).

For stationary configurations, the equivalent radial Klein-Gordon equation reads

$$P'' + \left( \frac{\nu' - \tilde{\lambda}'}{2} + \frac{2}{r} \right) P' = e^{\tilde{\lambda}} \left[ \frac{dU(P)}{dP^2} - e^{-\nu} \omega^2 \right] P, \quad (8)$$

where  $P := P(r) = \Phi(r, t) e^{i\omega t}$  is the radial function and  $U$  a self-interaction.

The decisive non-vanishing components of the Einstein equation are the ‘radial’ equations

$$\nu' + \tilde{\lambda}' = \kappa(\rho + p_r) r e^{\tilde{\lambda}}, \quad (9)$$

$$\tilde{\lambda}' = \kappa \rho r e^{\tilde{\lambda}} - \frac{1}{r} (e^{\tilde{\lambda}} - 1), \quad (10)$$

where  $\kappa = 8\pi G$  is the gravitational coupling constant in natural units. Two further components are identically fulfilled because of the contracted Bianchi identity  $\nabla^\mu G_\mu{}^\nu \equiv 0$  and the energy-momentum conservation (7).

One of the metric functions has the well-known exact parametric solution

$$e^{-\tilde{\lambda}(r)} = 1 - \frac{2GM(r)}{r} = 1 - \frac{\kappa M(r)}{4\pi r}, \quad (11)$$

where

$$M(r) := 4\pi \int_0^r \rho \tilde{r}^2 d\tilde{r} \quad (12)$$

is the Newtonian mass function at the distance  $r$  from the center.

## 3 DENSITY PROFILE OF NON-TOPOLOGICAL SOLITONS

As a solvable toy model (Mielke, 1978, 1979) with *self-interaction*, let us consider the Klein-Gordon equation (8) with a  $\Phi^6$  type potential

$$U(|\Phi|) = m^2 |\Phi|^2 (1 - \chi |\Phi|^4), \quad \chi |\Phi|^4 \leq 1, \quad (13)$$

where  $m$  is the ‘bare’ mass of the boson and  $\chi$  a coupling constant, which are thought of as constants of nature, cf. Mielke & Schunck (2002), Mielke, et al. (2002).

For a spherically symmetric configuration and the choice  $\omega = m$ , the corresponding nonlinear Klein-Gordon equation (8) simplifies in the limit  $\nu = \tilde{\lambda} \rightarrow 0$  of flat spacetime to an *Emden type equation*

$$P'' + \frac{2}{x}P' + 3\chi P^5 = 0, \quad (14)$$

which has the completely *regular* exact solution

$$P(r) = \pm \chi^{-1/4} \sqrt{\frac{A}{1 + A^2 x^2}}, \quad (15)$$

where we introduced the *dimensionless* radial coordinate  $x := mr$ , and  $A = \sqrt{\chi}P^2(0)$  is a free intergration constant depending on the central value  $P(0)$ . As is rather characteristic for *non-topological soliton* (NTS) solutions, its dependence on the nonlinear coupling parameter  $\chi$  is singular in the limit  $\chi \rightarrow 0$ .

From (6) we find in flat spacetime the energy density

$$\rho = \frac{2\rho_0}{2 - A^2} \left[ \frac{r_c^2}{r_c^2 + r^2} + \frac{A^2 r_c^4 (r^2 - r_c^2)}{2(r_c^2 + r^2)^3} \right], \quad (16)$$

where the central density of the NTS model  $\rho_0 = A(2 - A^2)m^2/2\sqrt{\chi}$  is positive for  $A < \sqrt{2}$  and the core or *scale* radius is  $r_c = 1/mA$ . For small  $A$ , the leading term of the Newtonian type mass concentration (16) is exactly the density law of the *quasi-isothermal sphere* (IS)

$$\rho_{\text{IS}}(r) = \rho_0 \frac{r_c^2}{r_c^2 + r^2}. \quad (17)$$

At large radii the density falls of like  $\rho \propto r^{-2}$  which corresponds to an asymptotically flat rotation curve. The NTS density (16) implies a *scaling law* for the dark haloes of the form

$$\rho_0 = \frac{m}{\sqrt{\chi}} \frac{1}{r_c} \left( 1 - \frac{1}{2m^2 r_c^2} \right) \simeq \frac{m}{\sqrt{\chi}} \frac{1}{r_c} \propto \frac{1}{r_c}, \quad (18)$$

where  $A$ , which may vary from halo to halo, *cancels out*. The remaining quotient  $m/\sqrt{\chi}$  may be tentatively regarded as universal constant of scalar dark matter (DM).

For  $r_c \gg 1/m$ , which is equivalently to  $\chi P^4(0) \ll 1$  and therefore within the positive range of the NTS self-interaction (13), the approximate scaling relation  $\rho_0 \propto 1/r_c$  has been successfully tested by Fuchs & Mielke (2004) against the observed properties of various types of galaxies.

Let us contrast these results with the density law of Navarro, Frenk & White (1996) based on simulations of conventional, i.e., non-interacting CDM: The corresponding generalized NFW profile

$$\rho_{\text{NFW}}(r) = \rho_0 \frac{r_c^3}{r^\epsilon (r_c + r)^{3-\epsilon}}, \quad 0 < \epsilon < 3. \quad (19)$$

is, however, singular with a cusp at the origin. The original NFW profile corresponds to  $\epsilon = 1$ . More realistic appears to be the empirical density profile

$$\rho_{\text{B}}(r) = \rho_0 \frac{r_c^3}{(r_c + r)(r_c^2 + r^2)}. \quad (20)$$

of Burkert (1995). It has a constant density core, similarly as the NTS halo, but a  $\rho \propto r^{-3}$  fall-off at infinity, similarly as the NFW profile.

#### 4 ROTATION CURVES

In general, for the static spherically symmetric metric (1), an observer at rest at the equator of the Schwarzschild type

coordinate system measures the following tangential velocity squared as a ‘point particle’ (a star or interstellar HI gas) flies past him in its circular orbit, *cf.* Misner *et al.* (1973), p. 657, Eq. (25.20):

$$\begin{aligned} v_\varphi^2 &:= e^{-\nu} r^2 \left( \frac{d\varphi}{dt} \right)^2 = \frac{1}{2} r \nu' = \frac{1}{2} \left[ 1 - e^{-\tilde{\lambda}} + \kappa p_r r^2 \right] e^{\tilde{\lambda}} \\ &\simeq \frac{\kappa}{2} \left[ \frac{M(r)}{4\pi r} + p_r r^2 \right]. \end{aligned} \quad (21)$$

As is well-known (Wald 1984), a naive application of the Newtonian limit would have led us to geodesics in flat spacetime, i.e. as if gravity would not affect the motion of test bodies like our stars moving in the DM halo. Thus it is mandatory to go beyond, as is indicated by our approximation of the generally relativistic formula (21). Then, also the pressure component  $p_r \neq 0$  of an anisotropic ‘fluid’ contributes, as is the case of scalar fields.

As our simplest fiducial example, we calculate the total mass

$$M(r) = 4\pi \rho_0 r_c^3 [r/r_c - \arctan(r/r_c)], \quad (22)$$

of the IS halo (17) which implies the corresponding circular velocity

$$v_\varphi^2 = \frac{\kappa}{2} \rho_0 r_c^2 \left[ 1 - \frac{r_c}{r} \arctan\left(\frac{r}{r_c}\right) \right]. \quad (23)$$

On the other hand, from the Newtonian NTS solution (15) and its radial pressure (6), we find the related rotation velocity

$$v_\varphi^2/v_\infty^2 = 1 + \left( \frac{A^2}{8} - 1 \right) \frac{r_c}{r} \arctan\left(\frac{r}{r_c}\right) + \frac{A^2 r_c^2 (r^2 - r_c^2)}{8(r_c^2 + r^2)^2}, \quad (24)$$

where

$$v_\infty^2 = \frac{\kappa \rho_0 r_c^2}{2 - A^2} \leq 10^{-6} \quad (25)$$

is restricted by observations.

According to Eq. (24) of the NTS model, the radial component  $e^{-\tilde{\lambda}}$  of the metric (1) asymptotically approaches the value  $1 - 2v_\infty^2 < 1$ . After a redefinition of the radial coordinate  $r \rightarrow \tilde{r} := r/\sqrt{1 - 2v_\infty^2}$ , the asymptotic space has a *solid deficit angle*: The area of a sphere of radius  $r$  is not  $4\pi r^2$ , but  $4\pi(1 - 2v_\infty^2)r^2$ . However, there is a remedy by identifying the boundaries of the deficit angle and thereby retaining an asymptotically flat metric, at the price of a conical singularity (Tod 1994) at the origin, similarly as in the case of cosmic strings, global monopoles and global textures, *cf.* Vilenkin & Shellard (1994).

The more *realistic* phenomenological Burkert fit (20) amounts asymptotically to a *logarithmic modification* of the Kepler law such that the velocity tends to zero at spatial infinity, with the consequence that *no* such deficit angle is to be expected.

#### 5 GRAVITATIONAL LENSING BY DARK MATTER HALOES

The lens equation *for large* deflection angles may be expressed as (Virbhadrha & Ellis 2000)

$$\tan \beta = \tan \theta - \frac{D_{\text{ls}}}{D_s} [\tan \theta + \tan(\hat{\alpha} - \theta)] \quad (26)$$

where  $D_{\text{ls}}$  and  $D_s$  are distances from the lens (deflector) to the source and from the observer to the source, respectively,  $\beta$  denotes the true angular position of the source, whereas  $\theta$  stands for the image positions. Observe that, for large angles, the distance  $D_{\text{ls}}$  cannot be considered a constant but it is a function of the deflection angle (Dabrowski & Schunck 2000).

One usually defines the reduced deflection angle to be

$$\alpha := \theta - \beta = \sin^{-1} \left( \frac{D_{\text{ls}}}{D_s} \sin \hat{\alpha} \right). \quad (27)$$

Since the gravitational potential  $|\phi| < 10^{-4}c^2$  of a galaxy is rather weak and neglecting pressure, one can use the linear approximation to Einstein's equations, for which

$$e^\nu \simeq 1 + 2\phi = 2 - n, \quad e^{\hat{\lambda}} \simeq 1 + 2r\phi' \quad (28)$$

holds in radial coordinates. Here  $n := 1 - 2\phi/c^2$  can be regarded as an effective refraction index in flat spacetime.

Then the Newtonian potential

$$\phi = -\frac{\kappa}{8\pi} \int \frac{\rho(\vec{r}')}{|\vec{r} - \vec{r}'|} d^3r', \quad (29)$$

as a solution of the Poisson equation via the method of Green's functions, is only determined by the energy density  $\rho$ . Accordingly, in this approximation the deflection angle is given by

$$\vec{\alpha}(\vec{r}) = - \int_0^s \vec{\nabla}_\perp n dl = 2 \int_0^s \vec{\nabla}_\perp \phi dl, \quad (30)$$

where  $dl \simeq dz$  is along the light path in an appropriately chosen coordinate system. For a geometrically-thin lens (Narayan & Bartelmann 1996), one usually considers the mass sheet orthogonal to the line-of-sight, commonly called the lens plane. It is characterized by its *surface mass density*

$$\Sigma(\vec{r}_\perp) = \int \rho(\vec{r}_\perp, z) dz, \quad (31)$$

where  $\vec{r}_\perp$  is a two-dimensional vector in the lens plane. The deflection angle at position  $\vec{r}_\perp$  is then the sum of the deflections due to all mass elements in the plane

$$\vec{\alpha}(\vec{r}_\perp) = \frac{\kappa}{2\pi} \int \frac{(\vec{r} - \vec{r}')_\perp \Sigma(\vec{r}'_\perp)}{|\vec{r} - \vec{r}'|_\perp^2} d^2r'_\perp. \quad (32)$$

In general, this deflection angle is a two-dimensional vector. In case of circular symmetry, the coordinate origin can be shifted to the center of symmetry and, so, light deflection is reduced to a one-dimensional problem.

Then the *dimensionless weak-field lens equation* can be written as

$$\beta(\theta) = \theta - \lambda \frac{g(\theta)}{\theta}, \quad \lambda := \frac{4\rho_0 r_c}{\Sigma_{\text{cr}}}, \quad (33)$$

where  $\theta = |\vec{r}_\perp|/D_l$  and  $\Sigma_{\text{cr}} = 2D_s/(\kappa D_l D_{\text{ls}})$  is the *critical surface density*. The function  $g$  is the normalized projected mass

$$\begin{aligned} M_\perp(r_\perp) &:= 2\pi \int_0^{r_\perp} du u \int_{-\infty}^{\infty} \rho(\sqrt{u^2 + w^2}) dw \\ &= 4\pi\rho_0 r_c^3 g\left(\frac{r_\perp}{r_c}\right) \end{aligned} \quad (34)$$

enclosed within a projected radius  $r_\perp$  and integrated along  $w := z/r_c$ . An *Einstein radius* is defined by the condition  $\beta(\theta_E) \equiv 0$ , or  $\theta_E^2 = \lambda g(\theta_E)$ .

For the IS halo, the normalized projected mass is given by

$$\begin{aligned} g_{\text{IS}}(x) &= \int_0^x u du \int_0^\infty \frac{dw}{1 + u^2 + w^2} \\ &= \frac{\pi}{4} \int_0^x \frac{du^2}{\sqrt{1 + u^2}} = \frac{\pi}{2} \left( \sqrt{1 + x^2} - 1 \right), \end{aligned} \quad (35)$$

where we applied for the evaluation of the improper integral the theorem of residues, and the corresponding bending angle is given by

$$\alpha_{\text{IS}}(x) = \frac{\kappa}{2} \rho_0 r_c^2 \frac{\sqrt{1 + x^2} - 1}{x}. \quad (36)$$

For the NTS profile, we similarly find

$$\begin{aligned} g(x) &= \frac{1}{2 - A^2} \left[ \pi \left( \sqrt{1 + x^2} - 1 \right) \right. \\ &\quad \left. + \frac{A^2}{2} \int_0^x du^2 \int_0^\infty \frac{u^2 + w^2 - 1}{(1 + u^2 + w^2)^3} dw \right] \\ &= \frac{\pi}{2 - A^2} \left[ \sqrt{1 + x^2} - 1 + \frac{A^2}{16} \int_0^x \frac{2u^2 - 1}{(1 + u^2)^{5/2}} du^2 \right] \\ &= \frac{\pi}{2 - A^2} \left[ \sqrt{1 + x^2} - 1 - \frac{A^2}{8} \left( \frac{1 + 2x^2}{(1 + x^2)^{3/2}} - 1 \right) \right]. \end{aligned} \quad (37)$$

In comparison, for the NFW profile the projected mass  $g(x)$  has been calculated by Bartelmann (1996), Zhang (2004) derived those of its generalizations (19), whereas Park & Ferguson (2003), discuss the weak and strong lensing regimes of the Burkert profile (20) for which  $\lambda_{\text{cr}} = 8/\pi$ .

## 5.1 Corrections due to pressure

A conserved symmetric energy-momentum tensor  $T_{\mu\nu}$  implies for the integrated spatial components the Laue theorem

$$\int T^{AB} d^3r = \frac{1}{2} \frac{d^2}{dt^2} \int T_{00} r^A r^B d^3r \quad (38)$$

in the limit of *flat* spacetime, cf. Sexl & Urbantke (1983, p. 78). Since the anisotropic stresses (6) of our NTS are *static*, they do not contribute to the gravitational potential  $\phi$  in this limit.

However, in a higher order approximation, the contribution from the radial pressure

$$p_r = \frac{A^3 m^2}{2\sqrt{\lambda}(1 + A^2 x^2)^2} = \frac{A^2 \rho_0}{2 - A^2} \frac{r_c^4}{(r_c^2 + r^2)^2} \quad (39)$$

of our NTS solution will cause a gravitational potential  $\tilde{\phi} := (e^\nu - 1)/2 \simeq \phi + \Psi$ , which is modified in comparison to the linear approximation (28) valid for configurations without pressure. Since the shift  $e^{\hat{\lambda}}$  is, according to the exact parametrization (11), only determined by the energy density  $\rho$ , its weak field approximation remains intact.

The modified gravitational potential  $\tilde{\phi}$ , entering now in the corresponding deflection angle (30), can readily be obtained by calculating the derivative  $\vec{\nabla}_\perp = 2\vec{r}_\perp \partial/\partial r^2$  perpendicular to the light path, but departing from the *general*

relativistic relation (21) for the rotation velocity:

$$\begin{aligned}\vec{\nabla}_\perp \tilde{\phi} &\simeq \frac{1}{2} \vec{\nabla}_\perp (e^\nu - 1) = \vec{r}_\perp r^{-2} v_\varphi^2 e^\nu \\ &= \frac{\kappa}{2} \vec{r}_\perp \left[ \frac{M(r)}{4\pi r^3} + p_r \right] e^{\nu+\lambda},\end{aligned}\quad (40)$$

in which the extra contribution from the radial pressure  $p_r$  becomes explicit.

Since  $e^{\nu+\lambda} \simeq 1$  as in the linear approximation and  $r dr = \sqrt{r^2 - r_\perp^2} dz$  in the choosen coordinate system, we find from Eq. (30) for the deflection angle of a NTS halo

$$\vec{\alpha}(\vec{r}_\perp) = 2\vec{r}_\perp \int v_\varphi^2 \frac{d \ln r}{\sqrt{r^2 - r_\perp^2}}. \quad (41)$$

In cases with a prescribed equation of state, Bharadwaj & Kar (2003) have discussed a similar relation between the deflection angle and the rotation velocity squared.

In this next order approximation, not only the normalized projected mass (34) but also the radial pressure  $p_r$  contributes via

$$\begin{aligned}p(x) &:= \frac{x^2}{\lambda} \int_{-\infty}^{\infty} p_r dz = \frac{A^2}{2 - A^2} \int_0^{\infty} \frac{x^2 dw}{(1 + x^2 + w^2)^2} \\ &= \frac{\pi A^2}{4(2 - A^2)} \frac{x^2}{(1 + x^2)^{3/2}} \\ &\rightarrow \frac{\pi A^2}{4(2 - A^2)} \frac{1}{x},\end{aligned}\quad (42)$$

to the bending angle, using the same normalization. In comparison to  $g(x)$ , the pressure contribution is negligible for small as well as large angles. In fact, the resulting  $\tilde{g}(x) = g(x) + p(x)$  is similar to the expression (38), only the term proportional to  $2x^2$  will disappear.

The corresponding lens equation (33) is drawn in Fig. 1 for different  $\lambda$ 's. Its shape is similar to that of the Burkert profile, cf. Park & Ferguson (2003), albeit for a different scale.

Eventually, more precise approximations would lead us to a general-relativistic treatment in which the nonlinear, gravitationally coupled KG equation (8) together with the full radial Einstein equations (9) and (10) need to be solved self-consistently, before the deflection angle (4) can be determined. Since the gravitational potential  $\phi$  of a galaxy is weak, we expect rather small corrections to the Emden type exact solution (15) from such numerical simulations, which are beyond the scope of the present paper.

Let us also remark that our model of a *self-gravitating* NTS is quite different from, e.g., brane-world scenarios (Harko & Cheng 2006), in which corrections to the Einstein equations are considered due to effective stresses induced by the projected Weyl curvature in the hypothetical bulk. Moreover, contrary to the ad-hoc assumption of Pal. et al. (2005), the IS type density (16) for the dark halo is an outcome of our NTS model.

## 6 DEMARCATION CURVES

Even for our weak field approximation of the gravitational field, one can distinguish between ‘weak’ and ‘strong’ lensing, depending whether or not the lense produces one or multiple images, cf. Bartelmann & Schneider (2001). This

depends on the characteristic value of the surface mass density. For the dimensions lens equation (33), the interval  $0 < \lambda \leq \lambda_{\text{cr}}$  is the range of ‘weak’ lensing, where the critical value  $\lambda_{\text{cr}}$  emerges from the condition  $d\beta/d\theta|_{\theta=0} = 0$  of a saddle point at the origin. Any lens-source combination with  $\lambda > \lambda_{\text{cr}}$  will produce multiple images.

Let us compare the critical values for different profiles:

$$\lambda_{\text{cr}} = \begin{cases} 0 & \text{NFW profile} \\ 16(2 - A^2)/[\pi(8 + 3A^2)] & \text{NTS with pressure} \\ 16(2 - A^2)/[\pi(8 - A^2)] & \text{NTS halo} \\ 4/\pi & \text{IS halo} \\ 8/\pi & \text{Burkert profile} \end{cases} \quad (43)$$

For  $0 < A < \sqrt{2}$ , the critical value of the NTS halo is larger than that of the NFW halo, but smaller than that of the isothermal sphere, assuming for  $A \rightarrow \sqrt{2}$  and  $A \rightarrow 0$  the corresponding limits. Consequently, the NTS halo, although exhibiting no density cusp at the center, can provide stronger lensing than the Burkert profile, irrespectively of the baryonic component.

Whereas deflection angles of galaxies still seem to be difficult to measure, *demarcation curves* can more easily distinguish between lensing scenarios with one or more images. Thus these strong demarcation lines could provide an independent means to probe the observational validity of different density profiles for dark matter haloes. For the NTS halo, there is only one image in the range  $0 < \lambda \leq \lambda_{\text{cr}}$ , beyond  $\lambda_{\text{cr}}$  gravitational lensing will produce three images.

It is remarkable that *constant*  $\lambda$  lines, in particular

$$\frac{4\rho_0 r_c}{\Sigma_{\text{cr}}} = \lambda_{\text{cr}}, \quad (44)$$

corresponds to the scaling relation

$$\rho_0 \propto r_c^{-1} \quad (45)$$

of DM haloes, which is parallel to the approximate scaling relation (18) predicted by NTS model. For ‘maximum disk’ models, it fits almost ideally astronomical observations (Fuchs & Mielke 2004). For Burkert haloes, Salucci & Burkert (2000) proposed the related *scaling relation*  $\rho_B(0) \propto r_c^{-2/3}$  on an empirical basis.

## 7 MAGNIFICATION AND TIME DELAY

The magnification of lensed images is given by

$$\mu = \left( \frac{\sin \beta}{\sin \theta} \frac{d\beta}{d\theta} \right)^{-1} \simeq \left( \frac{\beta}{\theta} \frac{d\beta}{d\theta} \right)^{-1}, \quad (46)$$

cf. Narayan & Bartelmann (1996). The tangential and radial critical curves (TCC and RCC, respectively) follow from the singularities of the tangential and the radial magnification

$$\mu_t \equiv \left( \frac{\sin \beta}{\sin \theta} \right)^{-1}, \quad \mu_r \equiv \left( \frac{d\beta}{d\theta} \right)^{-1}, \quad (47)$$

respectively.

Figure 3 shows the absolute value  $|\mu| = |(\theta/\beta)(d\theta/d\beta)|$  of the magnification of a NTS halo for several values of  $\lambda$ .

Let us also determine the Shapiro delay given by

$$\tau = 2 \int |\phi| dl = \frac{\kappa}{4\pi} \int \int \frac{\rho(\vec{r}')}{|\vec{r} - \vec{r}'|} d^3 r' dl. \quad (48)$$

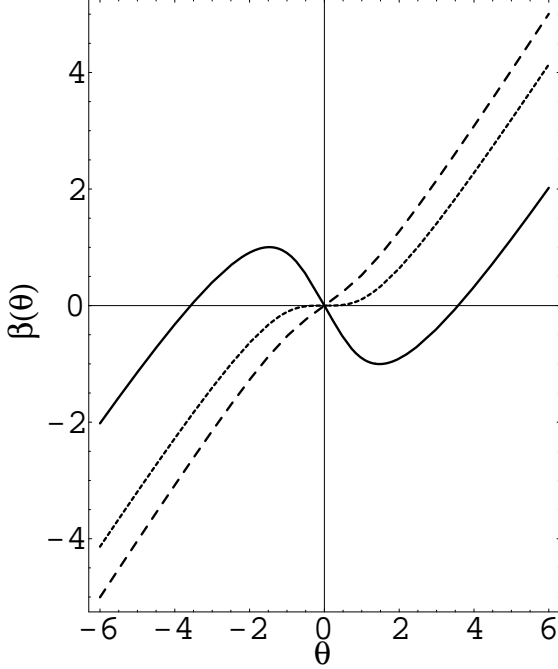


**Figure 1.** Dimensionless lens equation for the NTS halo with pressure for  $A = 0.805$ . The solid, dotted, and dashed lines are, respectively, for  $\lambda = 2$ ,  $\lambda_{\text{cr}}$ ,  $0.3$ . Multiple images occur for  $\lambda > \lambda_{\text{cr}} = 0.692428$ .

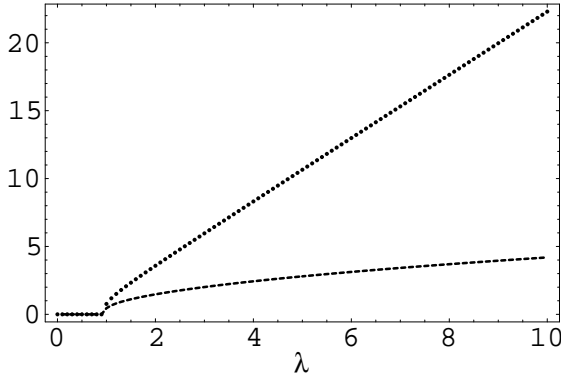


**Figure 2.** Values for Einstein rings (dotted line) and for the image separation ( $d\beta/d\theta = 0$ , dashed line), both for NTS haloes.

It is controlled dominantly by the Newtonian gravitation potential  $\phi$ , cf. Will (2003).

On the other hand, the reduced Shapiro delay  $\psi$  is the (super-)potential for the reduced deflection angle

$$\alpha(\theta) = \nabla_{\theta}\psi(\theta) = \lambda g(\theta)/\theta, \quad (49)$$

cf. Eq. (61) of Narayan & Bartelmann (1996). Thus we find equivalently,

$$\begin{aligned} \psi(\theta) &= \lambda \int_0^{\theta} g(x) d \ln x \\ &= \frac{\lambda\pi}{8(2-A^2)} \left\{ -8 - A^2 + 8\sqrt{1+\theta^2} + \frac{A^2}{\sqrt{1+\theta^2}} \right\} \end{aligned}$$

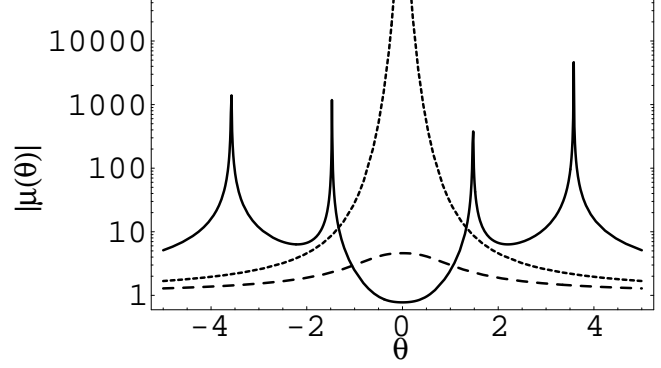


**Figure 3.** The magnification of a NTS lens. The solid, dotted, and dashed lines are, respectively, for  $\lambda = 2$ ,  $\lambda_{\text{cr}}$ ,  $0.3$ . The inner peak for  $\lambda = 2$  notifies the position of a radial critical curve, whereas the outer peak gives the position of the Einstein ring. (For the logarithmic representation, the absolute value of  $\mu$  is plotted. The magnifications between the singularities at both, positive and negative  $\theta$ , are actually negative.)

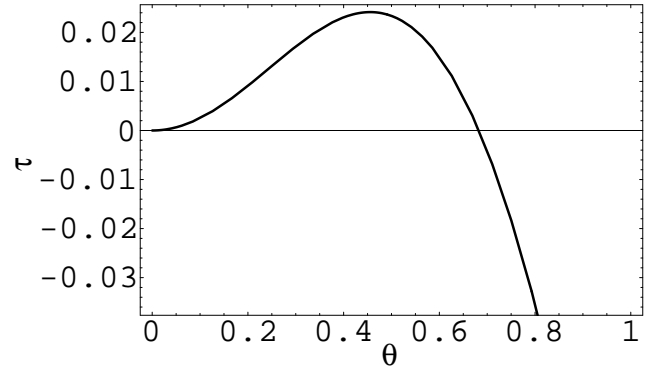


**Figure 4.** The reduced observed time delay  $\tilde{\tau} := (\theta - \beta)^2 - 2\psi$  as a function of  $\theta$  for  $A = 0.805$  and  $\lambda = \lambda_{\text{cr}}$ .

$$- (8 - A^2) \ln[(1 + \sqrt{1 + \theta^2})/2] \}. \quad (50)$$

[In the next order approximation  $\tilde{g}(x) = g(x) + p(x)$ , with the radial pressure of the NTS included, we would obtain the additional term  $\lambda\pi A^2(1 - 1/\sqrt{1 + \theta^2})/4(2 - A^2)$ .]

To the observable time delay

$$\Delta t = (1 + z_1) \frac{D_1 D_s}{2D_{\text{ls}}} [(\theta - \beta)^2 - 2\psi] \quad (51)$$

there contribute a geometrical part and the Shapiro delay, where  $z_1$  is the redshift of the lens. The result is shown in Fig. 4.

## 8 CONCLUSIONS

The lens properties of a solitonic scalar model of DM haloes reveal all qualitative features of a non-singular circularly symmetric gravitational lens. We derived the lens equation and plotted the corresponding curves, which turn out to be quite similar to those of the IS halo.

For a comparison with observations, the Castles survey

(Kochanek, et al. 2005) of 43 lenses with multiple images permits us to determine the observed parameter  $\lambda$  of the lens equation (33), i.e.

$$\lambda_{\text{obs}} = \frac{0.0057}{h} \frac{d_1 d_{\text{ls}}}{d_s} \frac{\rho_0 r_c}{M_{\odot} \text{pc}^{-2}}, \quad (52)$$

where  $h := H_0/100$  kpc is the normalized Hubble constant and  $d_1 := D_1 H_0/c$  etc. are dimensionless.

The angular diameters have been determined with the code of Kayser et al. (1997) adopting the parameters of the cosmological concordance model. The scaling relation (18) for the sample of galaxies studied by Fuchs & Mielke (2004) implies  $\rho_0 r_c \simeq 200 M_{\odot} \text{pc}^{-2}$ , if we use the minimum disk models. We find from (52), that  $\lambda_{\text{obs}} \leq 0.3$ , which implies that no multiple images would occur, if the DM haloes were modelled by the quasi-isothermal sphere (IS), for which  $\lambda_{\text{cr}} = 4/\pi$ . A similar finding was recently deduced from the CSL-1 candidate (Sazhin et al. 2003): The assumption of a DM filament (Fairbairn 2005) with density  $\rho < 300 M_{\odot} \text{pc}^{-2}$  is not sufficient in order to explain the presumably observed splitting of  $8.6 \times 10^{-6}$  radians.

However, for our NTS halo,  $\lambda_{\text{cr}}$  can approach zero as in the NFW case, whereas haloes modelled by the Burkert profile need an almost three times higher  $\lambda$  in order to produce strong lensing (Park & Ferguson 2003). This differences between the NTS model and the Burkert fit can be traced back to the fact that the NTS metric, as that of the related IS profile, corresponds to an asymptotically constant rotation velocity  $v_{\infty}$ . In a general relativistic setting, the space necessarily would exhibit a *deficit angle* of  $4\pi v_{\infty}^2$  or, equivalently, can be joined to a conical metric. Light passing a NTS halo simulating such a ‘cosmic string’ will be deflected by this deficit angle which, according to (25) has the right order of magnitude. Consequently, after removing the deficit angle by coordinate transformation, the linear mass density peaking at the location of the central coordinate ‘singularity’ of the conical metric would produce a splitting of images also for NTS haloes.

More recently, there are indications of a considerable *flattening* of dark halos from weak lensing observations (Hoekstra et al. 2004) of galaxies with a lower bound  $e_{\text{halo}} = 1 - c/a \geq 1/3$  on the observed halo ellipticity. Our Emden type scalar model has been probed (Mielke & Peralta, 2004) with respect to a possible ellipticity of exact NTS solutions, presumably due to rotation with angular momentum  $l$ , and round and flattened haloes are found, with an  $1/r^{2l+2}$  decay of the density at infinity. A ‘superposition’ of round and elliptic solitons to a halo with an effective  $l_{\text{eff}} = 1/2$  could be envisioned which would have the  $r^{-3}$  asymptotic decay of the density, familiar from the Burkert and NFW profiles. This idea, however, needs further study.

With respect to the core/cusp problem in low surface brightness galaxies, a new analysis by Gentile et al. (2004) has revealed that the Burkert curve – as any cored profile – has the best fits to the rotation curves of a new sample of five spiral galaxies. In general, the properties of DM haloes inferred from weak lensing (Hoekstra et al. 2004) provides a strong support for the existence of DM, whereas alternative theories of gravity, such as MOND, can almost be excluded.

## ACKNOWLEDGEMENTS

We would like to thank Fjodor Kusmartsev, Humberto Peralta, Remo Ruffini and Robert Schmidt for helpful discussions and comments. One of us (F.E.S.) acknowledges research support provided by a personal fellowship. Moreover, E.W.M. acknowledges the support of SNI and thanks Noelia, Markus Gérard Erik, and Miryam Sophie Naomi for encouragement.

## REFERENCES

- Bartelmann, M., 1996, *Astron. Astrophys.* 313, 697  
 Bartelmann, M., Schneider, P., 2001, *Phys. Rept.* 340, 291  
 Bharadwaj, S., Kar, S., 2003, *Phys. Rev. D* 68, 023516  
 Brans, C. H., Dicke, R. H., 1961, *Phys. Rev.*, 124, 925  
 Burkert A., 1995, *ApJ* 447, L25  
 Chwolson, O., 1924, *Astr. Nachrichten*, 221, 329  
 Cramer, C. R., 1997, *Gen. Rel. Grav.*, 29, 445  
 Dąbrowski, M. P., Schunck, F.E., 2000, *ApJ* 535, 316  
 Einstein, A., 1936, *Sci* 84, 506  
 M. Fairbairn, 2005, ‘‘CSL-1: Lensing by a Cosmic String or a Dark Matter Filament?,’’ arXiv:astro-ph/0511085.  
 Faraoni, V., 1993, *AA*, 272, 385  
 Fuchs, B., Mielke, E.W., 2004, *MNRAS* 350, 707  
 Fukugita, M., Futamase, T., Kasai, M., 1990, *MNRAS*, 246, 24  
 Gasperini, M., Veneziano, G., 1993a, *Mod. Phys. Lett.*, A8, 3701  
 Gasperini, M., Veneziano, G., 1993b, *Astroparticle Phys.*, 1, 317  
 Gentile, G., Salucci, P., Klein, U., Vergani, D., Kalberla, P., 2004, *MNRAS* 351, 903  
 Goodman, J, 2000, *New Astron.* 5, 103  
 Harko, T., Cheng, K. S., 2006, *Astrophys. J.* 638, 8  
 Hoekstra, H., Yee, H. K. C., Gladders, M. D., 2004, *ApJ* 606, 67  
 Jordan, P., 1959, *Z. Phys.*, 157, 112  
 Kayser, R., Helbig, P., Schramm, T., 1997, *Astron. Astrophys.*, 318, 680  
 Kochanek, C.S. et al., 2005, [http://cfa-www.harvard.edu /glens-data/](http://cfa-www.harvard.edu/glens-data/)  
 Mielke, E.W., 1978, *Phys. Rev. D* 18, 4525  
 Mielke, E.W., 1979, *Nuovo Cimento Lett.* 25, 424  
 Mielke, E.W., Schunck, F.E., 2002, *Phys. Rev. D* 66, 023503  
 Mielke, E.W., Schunck, F.E., and H.H. Peralta, 2002 *Gen. Rel. Grav.* 34, 1919  
 Mielke, E.W., H. H. Peralta, 2004 *Phys. Rev. D* 70, 123509  
 Misner, C.W., Thorne, K.S., Wheeler, J.A., 1973, *Gravitation* (W.H. Freeman, New York).  
 Narayan, R., Bartelmann, M., 1996, *Lectures on gravitational lensing*, preprint, astro-ph/9606001  
 Navarro J.F., Frenk C.S., White, S.D.M., 1996, *ApJ* 462, 563; *ApJ* 490, 493  
 Nordström, G., 1913, *Ann. Phys. (Leipzig)* 42,, 533  
 Pal, S., Bharadwaj, S., Kar, S., 2005, *Phys. Lett. B.* 609, 194.  
 Park, Y., Ferguson, H. C., 2003, *ApJ* 589, L65  
 Peitz, J., Appl, S., 1997, *MNRAS*, 286, 681  
 Petters, A. O., 2003, *MNRAS*, 338, 457  
 Salucci, P., Burkert, A., 2000, *ApJL* 537, L9  
 M. Sazhin et al., 2003, *MNRAS* 343, 353  
 Schneider, P., Ehlers, J., Falco, E. E., 1992, *Gravitational Lenses* (Springer, Berlin)  
 Schunck, F. E., Mielke, E.W., 1999, *Gen. Rel. Grav.* 31, 787  
 Schunck, F. E., Mielke, E.W., 2003, *Class. Quantum Grav.* 20, R301  
 Sexl, R.U., Urbantke, H.K., 1983, *Gravitation und Kosmologie* (Bibliographisches Institut, Mannheim)  
 Soldner, 1801, *Berl. Astron. Jahrb.*, 1804, 161; reprinted in *Ann. Phys.* 65 (1921) 593

- Spergel D.N., Steinhardt P.J., 2000, Phys. Rev. Lett. 84, 3760  
Tod, K.P., 1994, Class. Quantum Grav. 11, 1331  
Vilenkin, A., Shellard, E. P. S., 1994, *Cosmic Strings and Other Topological Defects* (Cambridge, Cambridge Univ. Press)  
Virbhadra, K. S., Narasimha, D., Chitre, S. M., 1998, AA, 337, 1  
Virbhadra, K.S., Ellis, G.F.R., 2000, Phys. Rev. D62, 084003  
Virbhadra, K.S., Ellis, G.F.R., 2002, Phys. Rev. D 65, 103004  
Wald, R.M., 1984, General Relativity (The University of Chicago Press, Chicago)  
Will, C. M., 2003 ApJ 590, 683  
Young, P., Gunn, J. E., Oke, J. B., Westphal, J. A., Kristian, J., 1980, ApJ 241, 507  
Zhang, T. J., 2004, ApJ 602, L5